MAIDEN TESTS OF THE HPT05 HELICON PLASMA THRUSTER PROTOTYPE

SPACE PROPULSION 2016, ROME, ITALY / 2–6 MAY 2016

Mario Merino [(1)], Jaume Navarro [(1)], Eduardo Ahedo[(1)], Víctor Gómez[(2)], Víctor Sánchez[(2)], Mercedes Ruiz[(2)] , Käthe Dannenmayer[(3)] , Eduard Bosch[(3)] , José González del Amo[(3)]

[(1)] Equipo de Propulsión Espacial y Plasmas (EP2), Universidad Carlos III de Madrid, Leganés, Spain. (mario.merino@uc3m.es)
[(2)] SENER Ingeniería y Sistemas, Tres Cantos, Madrid, Spain.
[(3)] Electric Propulsion Laboratory, ESTEC, ESA, Noordwijk, the Netherlands.

KEYWORDS: helicon plasma thruster

ABSTRACT:

A flexible 1 kW helicon plasma thruster prototype called HTP05 has been designed and built by SENER and EP2, with the aim of improving the present understanding of the physical mechanisms behind the operation of this device and assessing the worthiness of this technology for space propulsion. The first ignition of the HPT05 has been performed successfully at the EPL facilities at ESTEC, ESA in 2015. This document describes the HPT05 device and presents the upcoming test plans.

1. INTRODUCTION

The helicon plasma thruster (HPT) [1-3] is an innovative concept in electric propulsion that has attracted much attention in the last years due to its promising potential advantages, namely: (i) it is electrodeless, (ii) it accelerates the plasma contactlessly with its magnetic nozzle, (iii) it is adaptable and throttleable, potentially covering a wide thrust-Isp range (iv) it could easily use virtually any propellant besides xenon (v) it is compact and has a large thrust density (vi) it can be scaled to high powers. All these desirable characteristics would allow to build an adaptable, robust, compact and durable thruster with a rather simple power processing unit (PPU).

In spite of previous research efforts on the HPT technology, there is still a lack of a complete understanding of the operation of this device. Firstly, there is the plasma-wave interaction and electron heating by RF wave absorption. Secondly, ionization must take place to form a plasma. Then, the internal plasma dynamics dictates the plasma losses to the thruster walls and the plasma flux that enters the magnetic nozzle. Finally, the plasma is expanded by the divergent magnetic field, converting internal energy into directed kinetic energy and providing thrust. The plasma must detach successfully from the closed magnetic lines downstream. The driving loss mechanisms in the thruster are still poorly understood, and the current performance of helicon plasma thrusters is low (up to 10-15% in the best cases [2, 4]).

Building on the results of the ESA-funded project "Helicon Plasma Thruster for Space Missions," and upon our existing models for the ionization and internal plasma dynamics inside the helicon plasma source [5], the plasma-RF wave interaction [6], and the plasma expansion in the magnetic nozzle [7], a HPT prototype was designed and constructed jointly by EP2 and SENER in the 0.5-1 kW power range, and termed HPT05. The preliminary design and sizing of this device was presented in Ref. [8]. This development enables our consortium to perform tests on the HPT, with the aims of improving our understanding of the HPT physics, validating our physical models, and aiding in the optimization of the HPT technology.

The HPT05 prototype was tested for the first time in October 2015 at the EPL, ESTEC (ESA) facilities in The Netherlands, where its ignition, was preliminary investigated. Langmuir probes and emissive probes were used together with Faraday cups to measure plasma density, ion current, electron temperature and plasma potential at a distance of about 500-750 mm from the exit plane of the thruster. This paper reports on this preliminary experimental campaign and discusses the upcoming test campaign at EP2 laboratory in Madrid.

The rest of this document is structured as follows. Section 2 below presents the HPT05 design, highlighting its main characteristics. The experimental set-up at ESTEC is described in Section 3. Section 4 gathers the experimental results and discusses them. Finally, Section 5 contains the conclusions and a prospective of the future work with this device, including a brief description of the new electric propulsion laboratory at EP2 premises that will be used to continue the experimental investigation.

2. THE HPT05 HELICON PLASMA THRUSTER PROTOTYPE

The HPT05 prototype is designed to run primarily on argon, although it can easily run on other gases such as xenon. The HPT05 prototype consists of an assembly, whose physical parts are described

below, which has a total diameter of 230 mm and total length of 310 mm. A general sketch of the system is shown in Fig. 1 and a photograph of the assembled device in its present state can be seen in Fig. 2. Detailed dimensions and the nominal operating point of the device are presented in Table 1:

- A variable length cylindrical quartz tube that serves as the ionization chamber. A controlled aperture diaphragm can be optionally placed at the chamber exit to reduce the exit section area, and enhance neutral gas ionization.
- A half-helical copper antenna that surrounds the ionization chamber. This emits the required RF power to ionize the gas and heat the plasma.
- Two copper magnetic coils that generate an adjustable magnetic field on the discharge chamber. These coils are controlled independently with dedicated external power sources. The coils are wound around anodized aluminium spools and can be water-cooled using two external cooling jackets.
- An additional magnetic coil near the exit section of the discharge chamber generates the external magnetic nozzle (MN). It can be controlled independently with respect to the internal magnetic field system, and can be water cooled as well. Currently the MN shape is not optimized to provide a small plume divergence angle but to enable the study of the external plasma expansion.
- An injector head, made of Macor which houses the gas inlet tube and a diffusor injector. The injector head can be slid manually inside the quartz tube to change the chamber length. A cavity in the injector allows to insert a Neodymium permanent magnet to alter the plasma transport in the rear part of the thruster. The magnet was used in all of the tests.
- A supporting structure made of an aluminium back plate, holds all the elements with mounting rods.

Additionally, a dedicated, tuneable RF generator and power processing unit (RFGPU), capable of delivering up to 1 kW of RF power, and a flexible matching network were built to power the device. The RFG and matching network can operate at 6.78, 13.56 and 27.12 MHz, and are monotorized from a LabView interface. These two elements are shown in Fig. 3. The RFGPU is connected to the HPT05 helical antenna through a dedicated RF feed, passed into the vacuum chamber with an appropriate feedthrough.

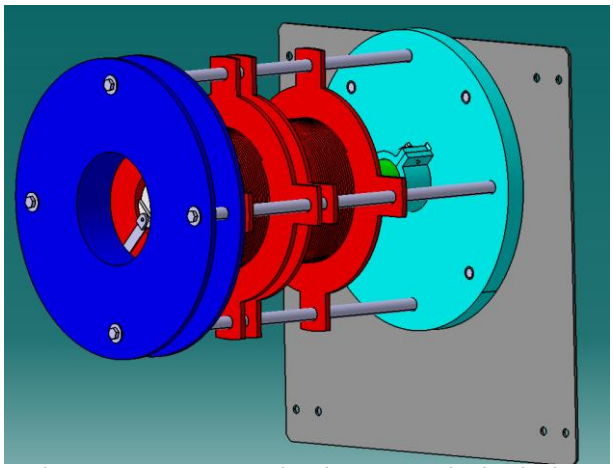

Figure 1. HPT05 CAD sketch. In cyan, the back plate and support structure; in red, the spools for the two magnetic coils that generate the internal magnetic field. In dark blue the spool of the magnetic nozzle. The quartz tube, antenna, and injector are contained within this assembly.

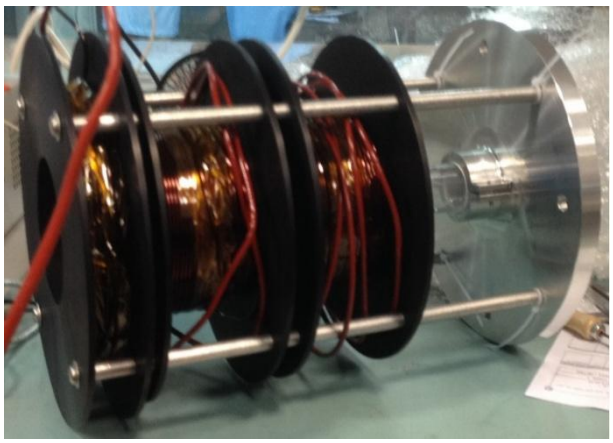

Figure 2. The assembled HPT05 plasma thruster prototype as-built.

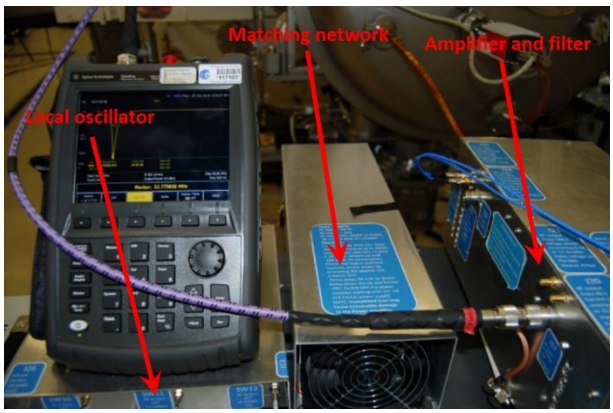

Figure 3. The RFG and matching network, together with a network analyser. The RFG is subdivided into a local oscillator and exciter circuit and a power amplifier stage.

Physical characteristics:	
Ionization chamber	Length: 100-250 mm (nominal: 150 mm); Inner radius: 15 mm
Antenna	Half-helical; 75 mm length
Internal field generator	Two copper coils on spools; 435 turns each Mean coil radius: 42.5 mm
Magnetic nozzle	Single copper coil on spool; 143 turns Mean coil radius: 61 mm
Propellant	Argon (other: xenon)
Operating range:	
Mass flow rate (Ar)	15-60 sccm (nominal: 50 sccm)
Power input at RF generator	200-1000 W (nominal: 800 W)
Magnetic field in chamber	0-600 G (nominal: 400 G)
RF frequency	6.78 – 27.12 MHz (nominal 13.56 MHz)

Table 1. HPT05 main physical parameters and operating range, with indication of the nominal operating point..

3. EXPERIMENTAL SET-UP

The preliminary test campaign of HPT05 took place in October 2015 at EPL facilities at ESTEC, ESA, in The Netherlands.

The CORONA vacuum chamber was used for the tests. CORONA [9] is a 2 m diameter, 5 m length chamber equipped with a 1 m diameter, 1.2 m length hatch for thruster mounting. CORONA has an oil-free pumping system with a pumping speed of 80000 l/s (Xe) that allows to operate at pressures better than 10^{-4} mbar at 5 mg/s (Xe). Although the performance of the cryogenic pumps is somewhat lower for argon (about 70000 l/s in total), background pressure was always lower than 2e-4 mbar in the tests. CORONA has a semi-circular 750 mm radius rotating arm onto which several probes can be mounted to take measurements of the plasma plume of the thruster.

A number of plasma probes from ESTEC Electric Propulsion Laboratory were employed to explore the plasma plume of the HPT05 during the first test campaign. This includes two simple Langmuir probes, eleven Faraday cups, and an emissive probe. These probes were mounted on the semi-circular rotating arm as shown in Fig. 4; their angular position is in Table 2. Faraday probe (FP) sensing surfaces were pointed to the thruster exit section centre and located at 880 mm from it.

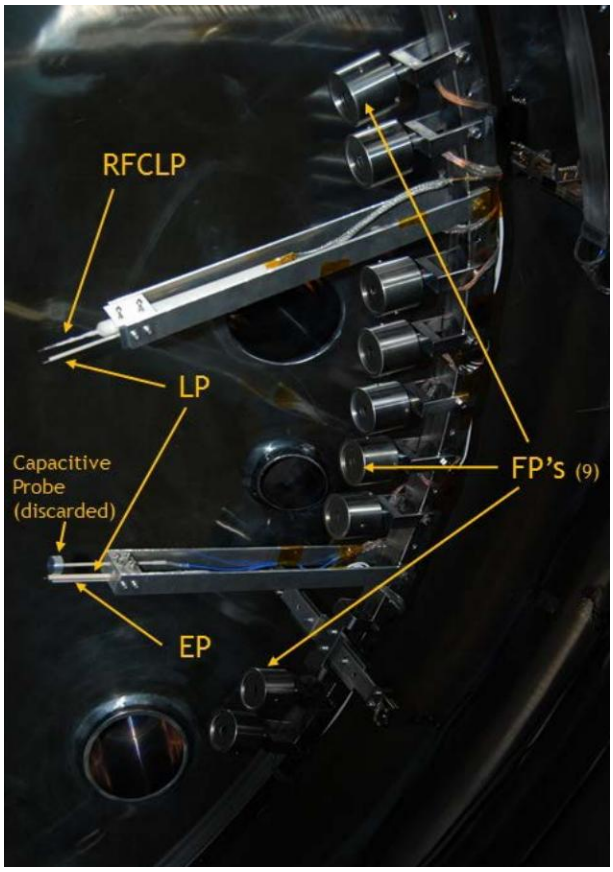

Figure 4. Plasma probes mounted on the semi-circular moving arm. The Langmuir probes (LP), the emissive probe (EP), and 9 of the 11 Faraday probes (FP) are visible. The discarded capacitive probe and the RF-compensated Langmuir probe are also shown.

Additionally, an experimental RF-compensated Langmuir probe and a capacitive probe were present in the set-up; unfortunately, a loose connection in the former and RF interference in the later prevented the utilization of these two diagnostics during the experiments.

Probe type	Angular position [deg]
FP 1	-75
FP 2	-32.5
FP 3	-27.5
RFCLP (discarded)	-15
LP 1	-15
FP 4	-10
FP 5	-5
FP 6	0
FP 7	5
FP 8	10
EP	15
LP 2	15
CP (discarded)	15
FP 9	20
FP 10	25
FP 11	75

Table 2. Description of the diagnostic system used for the preliminary HPT05 characterization test campaign at EPL, ESTEC.

Test #	DC power [W]	Mass flow rate [mg/s Ar]	$I_{coil1} = I_{coil2}$ [A]	I_{MN} [A]	Description and comments
Test12ND	189	1.19	7	10.5	Faraday cups
Test13ND	228	1.19	7	10.5	Faraday cups
Test14ND	245	1.19	7	10.5	Faraday cups
Test15ND	266	1.19	5	7	Faraday cups
Test16ND	322	1.19	7	7.6	Faraday cups
Test17ND	270	1.19	7	10.5	Faraday cups
Test18ND	228	1.19	7	10.5	Faraday cups
Test19ND	440	1.19	7	10.5	Faraday cups
Test20ND	600	1.19	8.7	13.2	Faraday cups
Test21ND	304	1.19	8.7	13.2	Full scan (all probes)
Test22ND	520	1.78	10.5	16	Faraday cups
Test23ND	320	1.78	10.5	16	Full scan (all probes)
Test24ND	320	1.48	10.5	16	Plasma cloud formed outside of thruster
Test25ND	378	0.89	10.5	16	Faraday cups + Langmuir probes

Table 3. Test case matrix. "ND" stands for "no diaphragm", as no diaphragm was used in these tests.

Several test cases were performed and multiple data sets were obtained in this first campaign with the different probes, mainly with the Faraday cups. The operating conditions for a selected subset of measurement are reported in Table 3. All these cases were run at 27.12 MHz. ND stands for no-diaphragm; a few test cases with a macor diaphragm that had a small aperture diameter of 150 mm were also carried out to check the effect of increasing the neutral density in the tube in the plasma generation process but are not reported here.

4. RESULTS

Remarkably, the thruster was ignited successfully after some initial troubleshooting with the water cooling system and the RFG. So far, only ignition at 27.12 MHz and 13.56 MHz has been achieved. Thruster operation was seen to be stable from an electrical and visual viewpoint. A picture of the running HPT05 can be seen in Fig. 5.

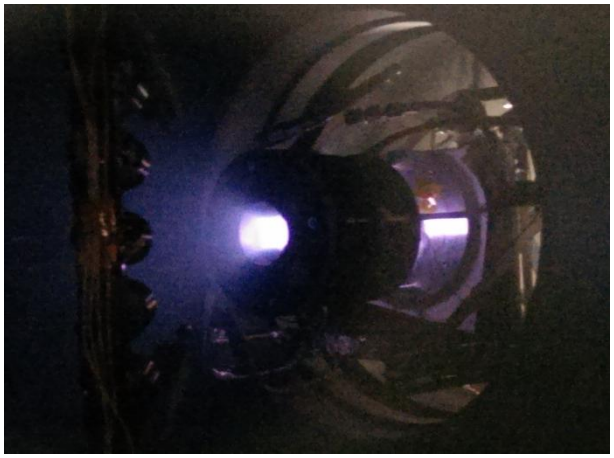

Figure 5. HPT05 in operation during a diagnostic sweep of the semi-circular rotating arm in the CORONA vacuum chamber.

A main limitation of the test campaign at ESTEC came from the partial malfunction of the RFGPU sensing system, which prevented us from obtaining a clear value of the resistive power delivered to the thruster. As a result, only the DC power fed to the RFGPU amplifier was known with certainty; accounting for the RFGPU efficiency losses and for a possible impedance mismatch, the power delivered to the thruster has been estimated to be around 35% or even lower, of the amplifier input power reported in Table 3. Later analyses on simulation models with the results recorded during the test campaign showed that electronic equipment best possible performance was not reached with the configuration selected in this experimental test campaign. Hence, the HPT05 was likely operated at a much lower power regime than the nominal one.

The array of Faraday cups was used to assess the ion current density in the plume and estimate the divergence angle and propellant utilization efficiency. Faraday probes 2, 5, and 11 did not provide valid readings and are disregarded in the analysis. Besides, FP 7 raw data presented a systematic offset that had to be corrected. Examples of raw FP measurements are provided in Fig. 6, and a postprocessed ion current density map can be seen in Fig. 7. The results of the measurements are reported in Table 4, where I_i is the (total) integrated ion current. From this table it is possible to see that plume divergence angle (computed as the central angle from thruster exit center point that covers 95% of the ion current) is about 70 deg or more, which agrees well with the expected values (the MN was not optimized for low divergence at this point).

The propellant utilization can also be estimated from these results,

$$\eta_u = \frac{m_i}{e}\frac{I_i}{\dot{m}} \qquad (1)$$

A very low value of the propellant utilization (below 1%) is found. This low utilization could be indicative of a poor RF power coupling and a low power deposition to the plasma, and/or an inadequate operating mode of the helicon source, probably operating in the low density inductive mode. The uncertainty on the delivered power to the plasma discussed above prevents the discussion of the prototype performance in this first experimental campaign. The next test campaign will remedy this (see Conclusions) and intends to clarify this point, obtaining actual performance figures of the thruster.

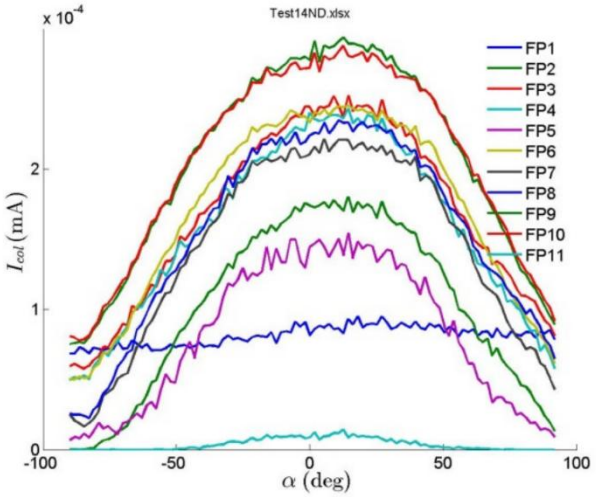

Figure 6. Collected ion current at the FPs as a function of the sweep angle α of the rotating arm. Data for test case number ND14.

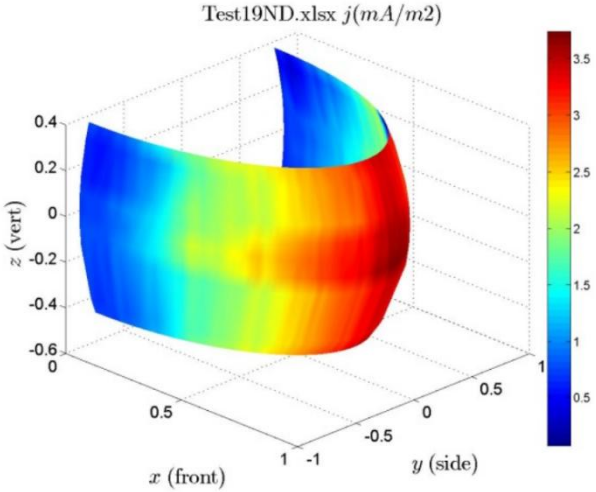

Figure 7. Computed ion current density map (mA/m^2) from the FP measurements in test case ND19.

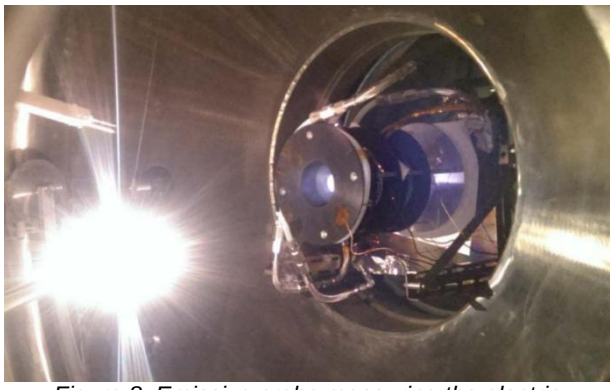

Figure 8. Emissive probe measuring the electric protential in the plasma plume during thruster operation

Test #	$\%I_i$ at 15 deg	$\%I_i$ at 30 deg	$\%I_i$ at 50 deg	$\%I_i$ at 70 deg	I_i [mA]
Test12ND	0.109	0.345	0.674	0.876	2.434
Test13ND	0.110	0.344	0.677	0.885	3.594
Test14ND	0.112	0.349	0.681	0.885	4.027
Test15ND	0.098	0.306	0.622	0.856	7.890
Test16ND	0.101	0.317	0.638	0.866	7.790
Test17ND	0.146	0.402	0.723	0.900	1.330
Test18ND	0.148	0.397	0.714	0.893	1.335
Test19ND	0.140	0.407	0.692	0.897	3.654
Test20ND	0.175	0.515	0.826	0.945	3.013
Test21ND	0.134	0.388	0.723	0.906	3.195
Test22ND	0.112	0.348	0.677	0.884	4.646
Test23ND	0.115	0.354	0.694	0.893	4.863
Test24ND	0.080	0.251	0.517	0.759	5.387
Test25ND	0.119	0.359	0.686	0.883	4.167

Table 4. Postprocessed plume ion current integrated from the axis up to a given angle, computed from the Faraday cup data.

Langmuir probe data was analysed with the standard probe theory (in OML regime) to estimate the plasma density, plasma potential, and electron temperature. This was only performed with a limited number of ND test cases; the summarized results of this investigation can be seen in Table 5. The estimated ion current density from these measurements (based on the sonic velocity of ions $c_s = \sqrt{T_e/m_i}$) agrees in order of magnitude with the current density level recovered from the FP measurements. Note that the low calculated density indicates a large Debye length compared to the probe size, challenging the validity of current LP calculations as a cylindrical probe in OML regime.

Finally, the emissive probe measurements were limited to two of these test cases due to time constraints in the test campaign. Under saturated emission conditions, the floating potential of the probe was measured and is reported in Table 5. A photograph of the EP during operation is presented in Fig. 8. Assuming a higher reliability on the EP potential measurements, it is clear that LP measurements underestimated the plasma potential by some volts.

Test #	LP1			LP2			EP
	T_e (eV)	ϕ_p (V)	n_i (m^{-3})	T_e (eV)	ϕ_p (V)	n_i (m^{-3})	ϕ_p (V)
Test21ND	4.2	24.6	$6.5 \cdot 10^{12}$	2.6	17.9	$1.6 \cdot 10^{13}$	30
Test23ND	4.0	20.5	$6.7 \cdot 10^{12}$	1.6	11.4	$1.8 \cdot 10^{13}$	22
Test25ND	4.2	21.4	$7.7 \cdot 10^{12}$	2.4	9.9	$1.1 \cdot 10^{13}$	N/A

Table XX. Postprocessed Langmuir and Emissive probe data. The preliminary computed values of electron temperature T_e, plasma potential ϕ_p, and ion density n_i are displayed.

In other test cases (not reported here), when the background pressure was higher than 10^{-4} mbar, secondary plasma creation by the RF wave was visible outside of the thruster chamber and the main plume, which could suggest the possible radiation of power by the antenna and the feeder cable in all directions. This source of inefficiency could be easily mitigated by the addition of a Faraday cage surrounding the antenna, a possibility that will be analysed in future work.

5. CONCLUSIONS AND FUTURE WORK

While this was a limited test campaign (in time and in quantity/quality of the measurements), the HTP05 test campaign at EPL can be considered a success. The maiden ignition of the HPT05 prototype was carried out smoothly just after a short series of attempts; a simple device start-up procedure was established; and preliminary data on the plasma plume was obtained.

The obtained results encourage us to continue the investigation of the HPT05, and reveal the main issues that require further work. Current thruster performance is likely very low, with a propellant utilization efficiency lower than 1% and an estimated plasma density at the source just above 10^{16} m^{-3}. Although the lack of detailed information about the power delivered to the antenna prevents us to carry out an adequate characterization of the prototype performance at this point, it is clear that there is a long way to improve the device performance up to a competitive level, and there is still much to understand about its operation. Further research will enable the optimization of the HPT05 attending to the lessons learned in this and future test campaigns, modelling, and simulation activities.

A key point of improvement in future work is related to the mentioned malfunction of the RFGPU auxiliary equipment, which proved an important drawback during the tests as it prevented the determination of the power delivered to the plasma, the plasma impedance, and the RF coupling. Without this information, an accurate characterization of the HPT05 performance was not possible. The lack of knowledge was mitigated a posteriori by using RFGPU simulations that confirmed the poor power transmission to the plasma.

Future work includes the continuation of the experimental investigation of the HPT technology at the new EP2 laboratory in Madrid. The upcoming test campaign to be started in late May 2016 will investigate in more detail the plasma plume characteristics, and conclude the analysis of the operational envelop of the present prototype. The test campaign intends also to provide recommendations on its improvement and information for the validation of the existing models and codes. A large dedicated vacuum chamber of 1.5 m diameter and 3.5 m long will be used with more than 30000 l/s (Xe) pumping speed provided by a combination of cryopanels and turbomolecular pumps allows to reach an ultimate vacuum pressure of 10^{-7} mbar and to run continuously for more than 5 days with a mass flow rate of 20 sccm Xe or Ar at $2 \cdot 10^{-5}$ mbar or better background pressure. More details on the characteristics of the vacuum chamber and the diagnostic systems that are being developed can be found on the EP2 website and on a companion poster in this conference [10].

ACKNOWLEDGMENTS

EP2 work has been supported by the Spanish Ministry of Economy and Competitiveness, Grant No. ESP2013-41052-P and grant UNC313-4E-1552, and ESA.

REFERENCES

[1] C. Charles, R. Boswell, and M. Lieberman, “Xenon ion beam characterization in a helicon double layer thruster,” Applied Physics Letters, vol. 89, p. 261503, 2006.

[2] O. Batishchev, “Minihelicon plasma thruster,” IEEE Transaction on Plasma Science, vol. 37, pp. 1563-1571, 2009.

[3] Mario Merino, et al. “Design and development of a 1kW-class helicon antenna thruster”. In 34th International Electric Propulsion Conference, IEPC-2015-297, OH, 2015

[4] K. Takahashi, A. Komuro and A. Ando “Effect of source diameter on helicon plasma thruster performance and its high power operation”, Plasma Sources Sci Tech 24, 055004, 2015

[5] E. Ahedo and J. Navarro, “Helicon thruster plasma modeling: Twodimensional fluid-dynamics and propulsive performances," Physics of Plasmas, vol. 20, p. 043512, 2013.

[6] B. Tian, E. Ahedo, and J. Navarro. “Analysis of plasma impedance in helicon antenna

thrusters". In 34th International Electric Propulsion Conference, number IEPC-2015-326, Fairview Park, OH, 2015

[7] E. Ahedo and M. Merino. Two-dimensional supersonic plasma acceleration in a magnetic nozzle. Physics of Plasmas, 17:073501, 2010.

[8] M. Merino, J. Navarro, S. Casado, E. Ahedo, V. Gómez, M. Ruiz, E. Bosch, J. González, "Design and development of a 1 kW-class helicon antenna thruster", presented at IEPC 2015 (IEP-C2015-297)

[9] J. Gonzalez del Amo, G. Saccoccia and P.E. Frigot, "ESA Propulsion Lab at ESTEC". In 31st International Electric Propulsion Conference, IEPC-2009-236, 2009.

[10] M. Merino, P. Fajardo, J. Navarro, X. Chen, Y. Babou, E. Ahedo, "Characteristics and capabilities of the new EP2 plasma propulsion laboratory", presented at Space Propulsion conference 2016, Rome, SP2016-3125013, 2016.